








Green Synthesis of Silver Nanoparticles Using Doxycycline: Evaluation of Antimicrobial Potential and Organ-specific Toxicity

Yasmin Akhtar^{1,2}, Ayoub Rashid¹, Muhammad Atif^{3*} , Sajjad Ullah⁴, Kiran Shehzadi¹, Tabinda Ijaz¹, Muhammad Ikram Ullah³ , Muharib Alruwaili³ , Abualgasim Elgaili Abdalla³ , Khalid Abosalif³ , Bi Bi Zainab Mazhari⁵  and Hasan Ejaz^{3*} 

¹Department of Chemistry, Government College University, Lahore, Pakistan.

²Department of Medical Laboratory Technology, University of Health Sciences Lahore, Pakistan.

³Department of Clinical Laboratory Sciences, College of Applied Medical Sciences, Jouf University, Sakaka 72388, Saudi Arabia.

⁴University Institute of Medical Laboratory Technology, Faculty of Allied Health Sciences, The University of Lahore, Lahore, Pakistan.

⁵Department of Clinical Laboratory Sciences, College of Applied Medical Sciences, Jouf University, Qurayyat 75911, Saudi Arabia.

Abstract

Silver nanoparticles (Ag-NPs) have wide applicability as antimicrobial, biomedical, and anti-cancer drug delivery systems. This study aimed to synthesize Ag-NPs using green methodology to assess their antimicrobial properties and toxicity. Ag-NPs were prepared using doxycycline, an antibiotic serving as a reducing and capping agent. The synthesized Ag-NPs were characterized by ultraviolet-visible spectrophotometry, X-ray diffraction, scanning electron microscopy, and Fourier-transform infrared spectrometry. The antimicrobial efficacy of doxycycline-mediated Ag-NPs was assessed on *Candida* species *in vitro* and for toxicity in male albino mice *in vivo*. The Ag-NPs showed a surface plasmon resonance at 411 nm, indicating a 90 nm average size and spherical shape. Toxicity was tested on mouse organs (liver, kidney, spleen, heart and stomach) using three Ag-NP doses (50, 100, 200 mg/kg) over 14 days. The synthesized Ag-NPs produced large inhibition zones against two well-known fungal species, *C. albicans* and *C. tropicalis*, demonstrating their antimicrobial potential. The Ag-NPs showed varying degrees of toxicity in different mouse organs, depending on the administered dose, with more pronounced adverse effects observed at higher concentrations. Periodic administration of Ag-NPs at low-dose volumes holds promise as a safe approach to their use as antimicrobial agents. Low-dose Ag-NPs are minimally toxic and show strong antimicrobial efficacy.

Keywords: Antimicrobial Activity, Ag-NPs, Toxicity, Green Method, *Candida albicans*, *Candida tropicalis*

*Correspondence: maahmad@ju.edu.sa; hetariq@ju.edu.sa

Citation: Akhtar Y, Rashid A, Atif M, et al. Green Synthesis of Silver Nanoparticles Using Doxycycline: Evaluation of Antimicrobial Potential and Organ-specific Toxicity. *J Pure Appl Microbiol.* 2024;18(4):2496-2506. doi: 10.22207/JPAM.18.4.21

© The Author(s) 2024. **Open Access.** This article is distributed under the terms of the [Creative Commons Attribution 4.0 International License](https://creativecommons.org/licenses/by/4.0/) which permits unrestricted use, sharing, distribution, and reproduction in any medium, provided you give appropriate credit to the original author(s) and the source, provide a link to the Creative Commons license, and indicate if changes were made.

INTRODUCTION

The synthesis of nanoparticles (NPs) or nanostructures (NSs) ranging in size from 1-100 nm, exploring their properties, and applications are part of a growing branch of nanotechnology. Nanochemistry and nanotechnology greatly interest researchers due to their relevance for almost all other research fields.¹ NPs and NSs are synthesized for their unique physical properties and chemical applicability to almost all physical and chemical processes, such as catalysis, photonics, electronics, and sensing, as well as to antibacterial or biomedical drug delivery.² This is because NPs/NSs offer greater surface-to-volume ratios and increased surface activity, leading to greater interaction of particles with the environment compared to their bulk forms.^{3,4}

Nanoparticles can be synthesized in two ways: in the bottom-up approach, atoms and small particles are aggregated to form NPs; and in the top-down method, bulk materials are broken down into particles in the nano range.⁵ Physical, biological and chemical techniques are used to synthesize NPs. Chemical methods employ toxic and expensive chemicals that often react at high temperatures and generate products hazardous to the environment.⁶ In contrast, biological or green methods utilize microbes or plants to synthesize cheap nanoparticles that are not hazardous to the environment and can be used at relatively low temperatures.^{7,8}

Fungal diseases caused by molds and yeasts are becoming a significant healthcare concern as modern medicine enables people with serious illnesses to live longer.⁹ Most antifungal drugs today are made from triazoles, polyenes, and echinocandins. However, some of these antifungals can cause problems, e.g., toxicity of amphotericin B, adverse reactions of azoles, and resistance to some antifungals.¹⁰ It shows antimicrobial resistance, rendering infections challenging to manage using conventional antifungal medications. As a result, it is critical to develop novel compounds that can be used to treat *Candida* infections while not harming host cells.

Silver and its compounds have been known since ancient times for their potent antimicrobial effects. Because of recent breakthroughs in metal

nanoparticle research, nano-Ag has attracted significant interest as a potential antibacterial agent.¹¹ Silver nanoparticles (Ag-NPs) are employed in antimicrobial applications, electronic components, and cosmetics. In order to develop new pharmaceutical products, uniform Ag-NPs with specific shapes, sizes, and other characteristics are of great interest to researchers.¹² As silver ions are toxic and highly hazardous to microbes, Ag-NPs have many antibacterial, antifungal, and inhibitory properties.¹³ Although the biocidal properties of Ag ions are well understood, the antifungal properties and mechanism of action of Ag-NPs are largely unknown.¹⁴ Zone inhibition is commonly used to estimate bactericidal and fungicidal activities of Ag-NPs.¹⁵ Membrane permeability and respiratory structures on the cell surface of microbes are known to be affected by Ag-NPs.¹⁶ Moreover, Ag-NPs can penetrate the cell and cause cell death depending on the dose administered.¹⁷

The selection of eco-friendly reducing and capping agents, suitable risk-free solvent media, and other non-hazardous chemicals is essential for the stability of Ag-NPs produced using green methods.¹⁸ Ag-NPs have been synthesized with β -D-glucose and starch as reducing and capping agents.¹⁹ Peng *et al.* synthesized Ag-NPs employing bamboo hemicelluloses and glucose for stability and as a reducing agent, respectively.²⁰ Ag-NP has been synthesized using a supernatant culture of *Bacillus licheniformis*.²¹ This method and other similar methods produce stable particles and have the advantage of using nonpathogenic microbes. Biological approaches to the synthesis of Ag-NPs often result in spherically shaped NPs. However, other nanostructures, such as nanospheres, nanorods, nanowires, nanopores, nanotriangles, and nanocapsules, have also been produced using biological methodology.²²

Our investigations were motivated by recent studies indicating the potential synergistic effects of biogenic Ag-NPs and various antibacterial and antifungal agents on *C. albicans* and *C. tropicalis*.²³ Our primary objective was to develop doxycycline-mediated Ag-NPs and evaluate their antifungal properties against *C. albicans* and *C. tropicalis*. In addition, a crucial aspect of our investigation involved the assessment of organ-specific toxicity of Ag-NPs at varying concentrations.

MATERIALS AND METHODS

Study design and ethical approval

We conducted a prospective study after obtaining ethical approval from the ethics committee of the Government College University, Lahore, Pakistan, in adherence to established ethical principles for animal research with ethical authorization number 255/CHEM/24.

Synthesis of silver nanoparticles

A 0.0008 M doxycycline solution (480.9 g/mol) was prepared by dissolving 38 mg of doxycycline in deionized water and adjusting the volume to 100 ml. A 0.8 mM solution of silver nitrate (AgNO_3) was prepared by dissolving 0.013 g of AgNO_3 in deionized water, with the volume made up to 100 ml in a volumetric flask. In addition, a 0.1 M sodium hydroxide (NaOH) solution was prepared by dissolving 0.4 g of NaOH in 100 mL of deionized water.

Five concentration ratios of AgNO_3 to doxycycline were prepared and tested to obtain the best results. Different ratios (1:1, 1:2, 1:3, 1:4, and 1:5) of doxycycline antibiotic and Ag^+ ions were formulated with the same concentration of an aqueous solution of doxycycline and AgNO_3 (0.8 mM/0.0008 M). Doxycycline was added to AgNO_3 at various ratios and then 0.1 M NaOH was added to maintain the pH of the reaction mixture. The solutions were placed in sunlight for 60 minutes, resulting in the reaction mixture's color changing from that of the extract to brown. The reduced metal particles were measured using Cary 60 ultraviolet-visible (UV-Vis) spectrophotometer (Agilent, Santa Clara, USA) at different intervals. Doxycycline was used as a stabilizing, capping, and reducing agent.

Characterization of silver nanoparticles

The reaction between doxycycline (colorless) and AgNO_3 (colorless) produced Ag-NPs indicated by a change in the color to brown. NPs reduced by doxycycline were measured using a UV-Vis spectrophotometer to detect nanoparticle formation. The morphology of antibiotic-mediated Ag-NPs was studied using scanning electron microscopy (SEM; Carl Zeiss AG, Oberkochen, Germany) under an acceleration voltage of 20 KeV. Functional group analysis of doxycycline and

Ag-NPs was performed with a Fourier-transform infrared spectrometer (FTIR; FT-IT-8900, Shimadzu Corporation, Kyoto, Japan) at 75°C within the wavenumber range of 400-4000 cm^{-1} . X-ray diffraction (XRD) analysis of the Ag standard and doxycycline-induced Ag-NPs was performed using an X-ray diffractometer D8 DISCOVER (Bruker Corp., Billerica, USA).

Antimicrobial assay of silver nanoparticles

The antimicrobial activity of doxycycline-mediated Ag-NPs was tested on colonies of *C. albicans* and *C. tropicalis*. Mueller-Hinton agar was used for all antimicrobial assays.²⁴ The antimicrobial characteristics of Ag-NPs were analyzed using the well-diffusion method at pH 7. A sterile cotton swab was dipped into each microbial inoculum at a standardized concentration (0.5 McFarland turbidity) and then streaked on an agar plate to obtain approximately 10^7 cells. Then, five holes, 3 mm in size, were punched aseptically in the culture plate surface; the wells thus created were loaded with 100 μl of Ag-NPs (25, 50, and 80 $\mu\text{g}/\text{mL}$), a positive control with doxycycline and the negative control with deionized water at pH 7. The inoculated plates were incubated at 37°C for 36 hours, after which the inhibition zones of microbial colonies were observed.

Silver nanoparticle toxicity assays with mice

In vivo toxicity studies of Ag-NPs were performed with male albino mice (*Mus musculus*) with a body weight of 25-30 g. The mice were obtained from the Veterinary Research Institute, Lahore and were kept at 50-70% humidity and $25 \pm 2^\circ\text{C}$ temperature. *Mus musculus* were fed with rodent pellets and tap water. Three groups of mice were orally administered Ag-NPs at 50, 100, or 200 mg/kg, while the fourth group was kept as the control without administration of Ag-NPs.

The mice were sacrificed after 14 days of repeated oral administration of Ag-NPs, and their organs were removed for tissue processing. Hematoxylin and eosin were used for the staining of tissue samples and then visualized microscopically. Slides of the organs of mice in the control group were microscopically imaged and compared with those of mice administered Ag-NPs at 50, 100, and 200 mg/kg.

RESULTS

Characterization of silver nanoparticles

The maximum lambda of the standard doxycycline solution was observed at 374 nm, while that of Ag-NPs was observed at 413 nm (Figure 1). The homogenized doxycycline-Ag-NPs had a spherical shape and their average size was 90 nm (Figure 2).

Infrared spectra yield critical insights into the organic compounds located on the surface of NPs. The FTIR spectra identified the functional groups and unique transmittance peaks of each component associated with the production of NPs. The FTIR spectra of doxycycline presented stretching peaks of OH at 3576 cm^{-1} related to alcohols and phenols, NH (amines) at 3281 cm^{-1} representing the stretching vibrations of carbonyl

groups of proteins, CH at 2988 cm^{-1} resulting from the asymmetric stretching of alkanes, CO at 1700 cm^{-1} representing the stretching vibrations aromatic compounds, and amide carbonyl at 1600 cm^{-1} , whereas in the case of Ag-NPs, the stretching peaks of OH shifted to 1416 cm^{-1} (shown in the spectrum in black in Figure 3), which represented doxycycline capped to silver atoms, indicating Ag-NP synthesis.

X-ray diffraction spectroscopy was used to study Ag-NPs at 30 kV voltage and 20 mA current, and the scanning rate was 0.05 $^{\circ}\text{C}/\text{min}$ in two hours for the range of 200 $^{\circ}$ -800 $^{\circ}\text{C}$. The Scherrer equation ($D \approx 0.9\lambda / b\cos \theta$, where D = crystal size, λ = X-ray wavelength, b = width of radiation peak, and θ = Bragg's angle) was used to determine the crystalline size of nanoparticles (Figure 4). The XRD diffraction peaks for Ag-NPs at 2θ values of

Table. Measurement of zones of inhibition (mm) caused by the antimicrobial activity of Ag-NPs against colonies of *Candida albicans* and *Candida tropicalis*

Microorganism	Diameter of inhibition zone (mm)				
	Negative control	Doxycycline	Ag-NP concentration ($\mu\text{g}/\text{mL}$)		
			25	50	80
<i>C. albicans</i>	0	17	0	12	17
<i>C. tropicalis</i>	0	17	9	12	18

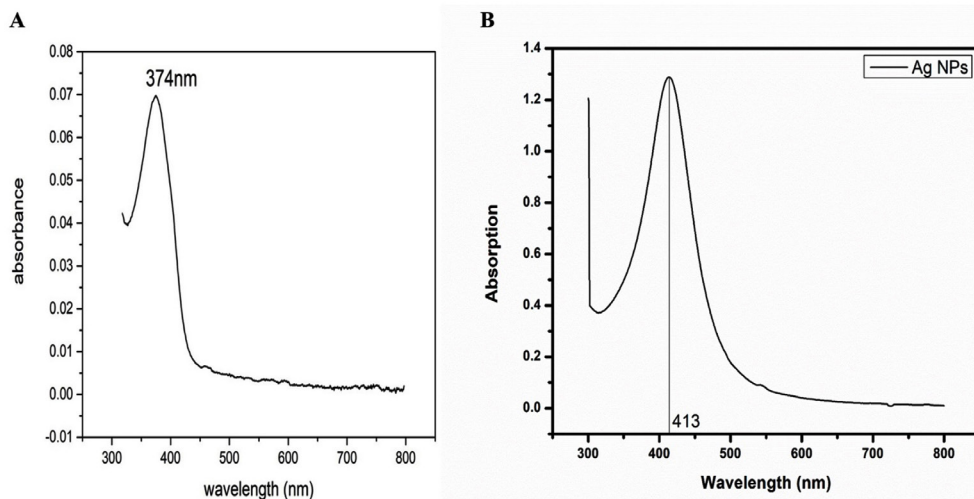


Figure 1. Ultraviolet-visible (UV-Vis) spectroscopic analysis of doxycycline. (a) The UV-Vis spectrum of doxycycline shows a prominent absorption peak at 374 nm (λ_{max}). (b) The UV-Vis spectrum of doxycycline after capping with silver nanoparticles (Ag-NPs) shows a distinct shift in λ_{max} to 413 nm, indicating successful encapsulation of doxycycline by Ag-NPs

38.49°, 44.29°, 64.45°, and 77.59°. These distinct peaks arise from the presence of Ag-NPs, leading to differences in the X-ray diffraction pattern. The observed peaks correspond to the (200), (200), (101), and (101) crystallographic planes, respectively, showing a crystal structure of face-centered cubic (FCC) typical of metallic silver.

Antimicrobial applications

The comparison of the zones of inhibition (diameter in mm) between the various concentrations of Ag-NPs, the negative control

(deionized water), and the positive control (doxycycline) (Table and Figure 5) showed that Ag-NPs had excellent antimicrobial action against *C. albicans* and *C. tropicalis*.

Histopathological examination of the toxicity of Ag-NPs in mice

Histopathological studies of group 1 (control) mice, which were not given any Ag-NPs, showed normal tissue and cellular structure in the stomach, lung, liver, kidney, and heart (Figure 6A). Histopathological studies of group 2

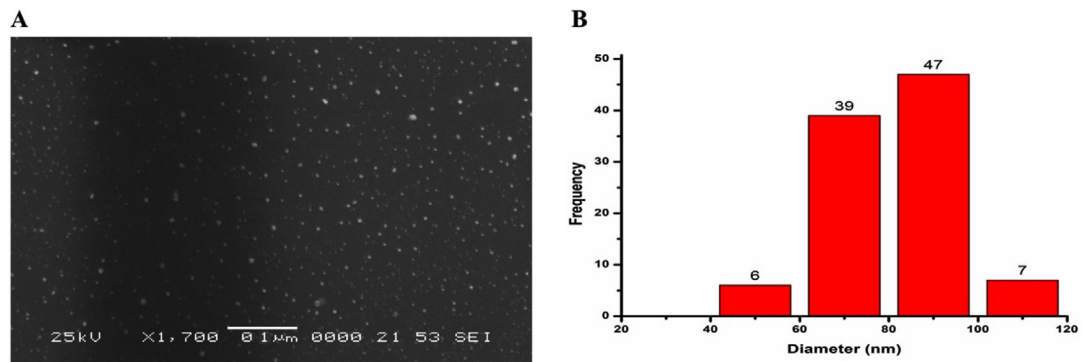


Figure 2. Size estimation and morphological characterization of Ag-NPs. (a) Scanning electron microscopy analysis reveals the spherical shape of the Ag-NPs, with an average size of 90 nm. (b) According to particle analyzer results, most Ag-NPs induced by doxycycline fall within 40-90 nm

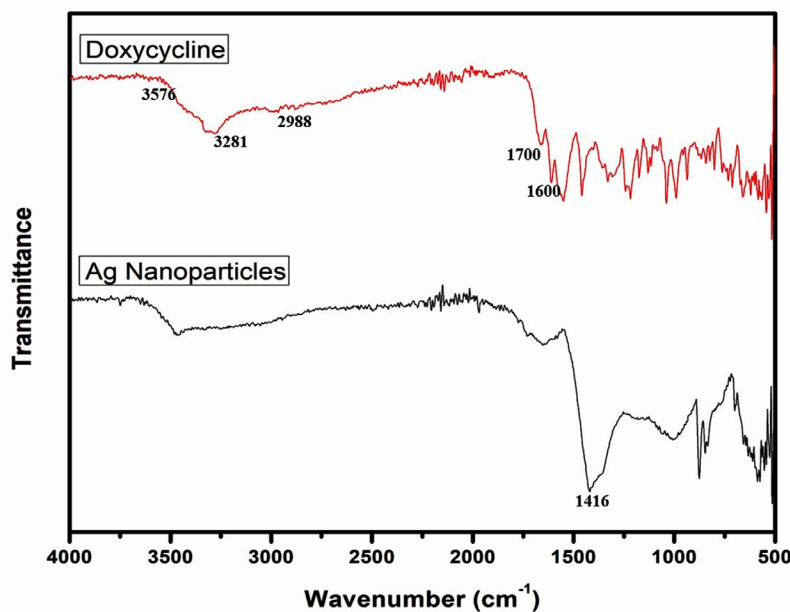


Figure 3. Fourier-transform infrared spectrometer spectra of doxycycline and Ag-NPs showing different peaks

mouse organs after exposure to 50 mg/kg doses of Ag-NPs found slight toxicity indicated by minor erosion and distortion of the stomach lining; inflammation, neutrophils (1+), lymphocytes (1+), and a low level of vascular conjunction in lung tissue; edema, inflammation, and Pyknosis (degenerative changes) (1+) in liver tissue; and minor vascular congestion in kidney tissue, but no signs of toxicity in heart tissue (Figure 6B).

Histopathological studies of group 3 mouse organs after exposure to 100 mg/kg doses of Ag-NPs showed abnormalities in stomach tissue indicated by moderate erosion (2+) and thinning of the mucosal wall with 2% inflammation; abnormality in lung tissue indicated by inflammatory edema (1+) and lymphocytes (2+); effects of toxicity on liver tissue indicated by periportal inflammation (1+), necrosis (1+), edema

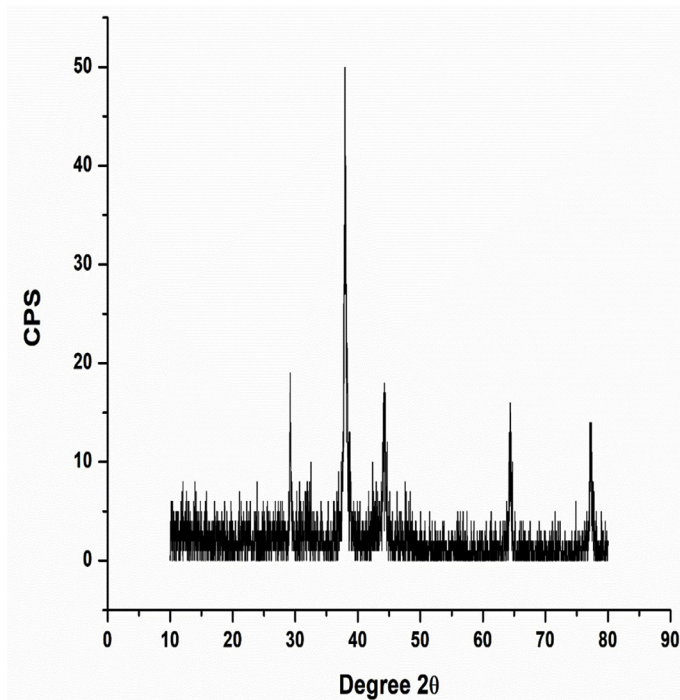


Figure 4. X-ray diffraction pattern of Ag-NPs synthesized with doxycycline

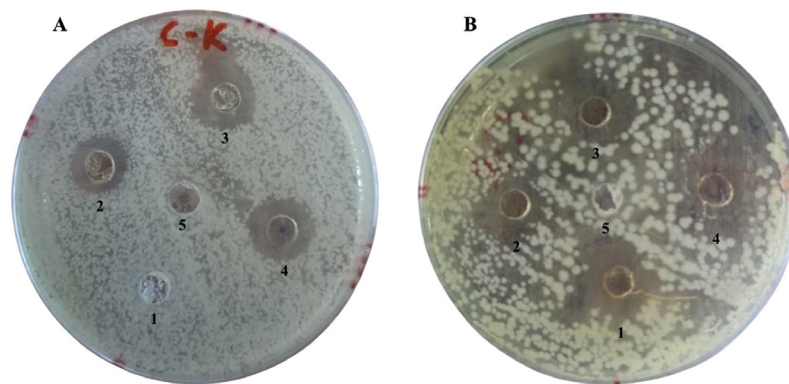


Figure 5. Zones of inhibition of colonies of (a) *Candida albicans* and (b) *Candida tropicalis* treated with doxycycline-coated silver nanoparticles (Ag-NPs). The numbers 1, 2, and 4 in both figures refer to Ag-NP concentrations of 25, 50, and 80 µg/mL, respectively; 3 is the positive control (doxycycline), and 5 is the negative control (deionized water)

(1+), karyorrhexis and pyknosis of the nucleus, and vascular conjunction; and toxic effects of Ag-NPs on kidney tissue indicated by up to 30% shrinkage of glomerular cells, while heart tissue showed normal structure and no signs of toxicity (Figure 6C).

Histopathological studies of group 4 mouse organs after exposure to 200 mg/kg of Ag-NPs showed signs of ulceration in stomach tissue, thinning of the mucosal lining and epithelium wall and a decrease in the number

of glands, and degraded stomach structure; toxic effects on lung tissue indicated by a pneumonic patch of lymphocytes (2+), inflammation, and hyperplasia; effects of toxicity on liver tissue indicated by vascular congestion, periportal inflammation (3+), edema (3+), pyknosis and karyolytic changes (2+), and liver necrosis (2+); and toxic effects on kidney tissue indicated by a 40% decrease in the size of glomerular cells and tubular necrosis (1+); and heart tissue with normal structure showing no signs of toxicity (Figure 6D).

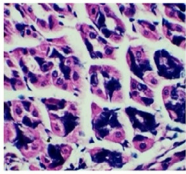
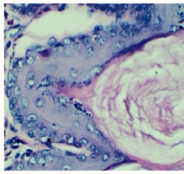
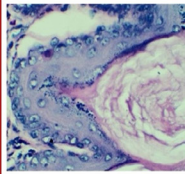
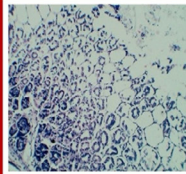
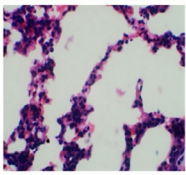
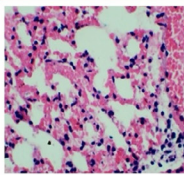
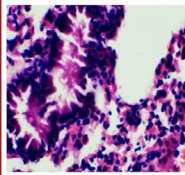
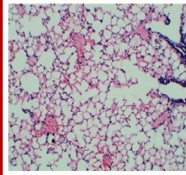
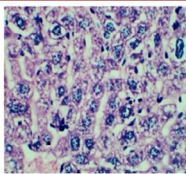
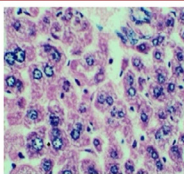
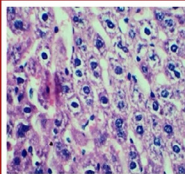
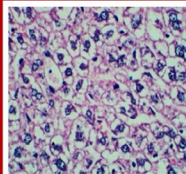
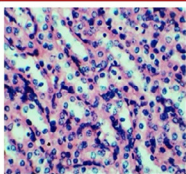
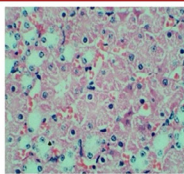
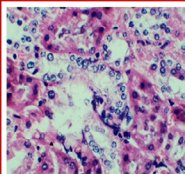
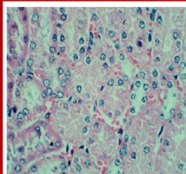
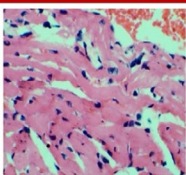
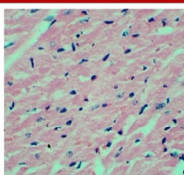
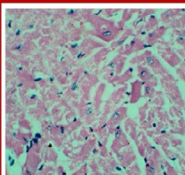
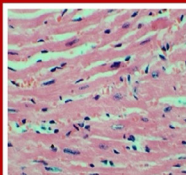
Organ Type	A Group 1 (Control)	B Group 2 (50 mg/kg)	C Group 3 (100 mg/kg)	D Group 4 (200 mg/kg)
Stomach				
Lung				
Liver				
Kidney				
Heart				

Figure 6. Comparative histopathological examination of four groups of mice exposed to different doses of Ag-NPs. Histological changes in various organs, including the stomach, lungs, liver, kidneys, and heart tissue, corresponding to the Ag-NP dose administered, are shown. (A) Group 1: No Ag-NP dose administered, organs showing baseline histological characteristics; (B) Group 2: 50 mg/kg of Ag-NPs administered; (C) Group 3: 100 mg/kg of Ag-NPs administered; and (D) Group 4: 200 mg/kg of Ag-NPs administered

DISCUSSION

Inorganic nanoparticles have become crucial to the production of innovative nanodevices employed in various biomedical, biological, physical, and pharmaceutical applications. Nano-Ag is extremely lethal to many microbes and prevents their growth, except for a few strains that show resistance.¹⁴ This study aimed to synthesize Ag-NPs and test their antifungal efficacy against *C. albicans* and *C. tropicalis*. We synthesized antibiotic-mediated Ag-NPs using a wet chemical reduction technique. Size-controlled particles were synthesized by optimizing reaction conditions.

In this study, doxycycline-Ag-NPs were synthesized within 60 minutes in sunlight with a surface plasmon resonance (SPR) band of 411 nm. In previous studies, the SPR of Ag-NPs was mostly 350 to 420 nm,²⁵ which matches our UV-Vis results. SEM displayed that the morphology of homogenized particles was spherical and 90 nm in size. The specified nanoparticle size for SEM must be 1-100 nm.²⁶ In FTIR, the stretching peaks of OH were at 3400 cm⁻¹, which are broadband, NH were at 3166 cm⁻¹, CO at 1699 cm⁻¹, and CH at 2966 cm⁻¹, in which the peak was shifted from 1550 to 1350 cm⁻¹.²⁷ The stretching peaks of our synthesized Ag-NPs were OH = 3576 cm⁻¹, NH = 3281 cm⁻¹, CH = 2988 cm⁻¹, CO = 1700 cm⁻¹, and amide carbonyl = 1600 cm⁻¹, which shifted to 1416 cm⁻¹, demonstrating that doxycycline capped to silver. XRD results indicated diffraction at 2θ = 38.29°, 44.39°, 64.55°, and 77.69°.²⁸ However, the XRD diffraction pattern of antibiotic-mediated Ag-NPs showed that 2θ = 38.49°, 44.29°, 64.45°, and 77.59°, indicating that there was no oxide formation and that Ag-NPs were produced.

Silver nanoparticles showed a good zone of inhibition against microbes depending on concentration and size. The antimicrobial action of our doxycycline-Ag-NPs was good, with a 17-mm maximum zone of inhibition. There are few studies on how Ag-NPs enter fungal cells, but it remains an intriguing question that needs further investigation, as does the structure of the fungal cell wall. We propose that the uptake of Ag-NPs may include endosomal trafficking systems that contribute to the absorption and release of nutrients and macromolecules. Macromolecules

and synthetic nanoparticles are transferred across the cell wall by fluid-phase endocytosis, a form of endocytosis, as shown by the assimilation of an impermeable dye, Lucifer yellow, into the vacuole by *C. albicans*.¹⁴

By being able to rupture cell membranes and prevent regular cell division, Ag-NPs are remarkably effective as anticandidal agents against *C. albicans*.²⁹ Additionally, the breakdown of membrane-bound lipids and enzymes results in lysis of the cells, which increases the effectiveness of Ag-NP anticandidal treatment by generating insoluble substances with sulfhydryl groups in *Candida* cell walls.³⁰ It also leads to a decrease in membrane permeability, which causes potassium ions to leak out of *Candida*.³¹ These Ag-NP-induced processes lead to *Candida*'s cell death by altering cell permeability, interfering with DNA replication, and preventing the synthesis of proteins.³² Smaller particles penetrate the cell, produce more reactive oxygen species, and injure tissue and cells more than larger particles in the range of 100 nm.

Kadam *et al.* in 2024 performed a study involving *F. schweinfurthii* bio templates under sunlight and microwave catalysis, showing an eco-friendly approach for synthesizing Ag-NPs. The plant-derived extracts (PAE and CAE) act as reducing and capping agents, transforming Ag⁺ ions into Ag-NPs, under varying pH, temperature, and catalyst exposure. They optimized the microwave conditions by adjusting exposure time and reagent concentrations which accelerates the reaction, enhancing nanoparticle yield and stability. The antimicrobial assay performed on these NPs proved the efficacy of these NPs *in vitro* experiments against clinical bacterial isolates.³³

In other similar study, Rizwana *et al.* in 2022 utilized a natural extract (red currant) for sunlight-mediated synthesis of Ag-NPs within a short time frame of 9 minutes. This rapid synthesis was attributed to the natural antioxidants and biomolecules in the extract, facilitating the reduction of silver nitrate (AgNO₃) to Ag-NPs. These NPs were found to be highly effective in inhibiting the growth of some bacterial and fungal isolates.³⁴

We studied the histopathology of four groups of mice to monitor the toxicity of Ag-NPs. Different doses of Ag-NPs were given orally and allowed to penetrate cell walls, causing an abrupt

rise in oxidative stress and cell death. The group of mice dosed with 50 mg/kg showed slight signs of toxicity. In contrast, the signs of toxicity were stronger in the mice given 100 mg/kg doses of Ag-NPs as indicated by distortions and abnormality in organ structures. The group of mice given 200 mg/kg doses showed a significant level of toxicity as indicated by the ulceration, rupturing, and thinning of walls in addition to structural distortions.

Silver nanoparticles produced by numerous methods have been described to be toxic as they can reach and accumulate in almost all organs, like the stomach, lungs, liver, kidney, spleen, and even the brain, depending on how they enter the body. Ag-NPs subcutaneously administered to rats are translocated to the brain, lungs, kidneys, liver, and spleen.³⁵ When used at high concentrations, Ag-NPs are lethal, cause membrane leakage of lactate dehydrogenase, and generate a significant amount of reactive oxygen species, ultimately leading to cell death.³⁶ Human cells with lung cancer exposed to Ag-NPs loaded with dyes showed signs of toxicity.³⁷ The toxicity of Ag-NPs has also been investigated based on different coatings. As Ag-NPs have considerable applicability in biokinetic processes, evidence of their toxicity is important and necessary to determine their mechanism of action in organs and effects on bodily functions.³⁸

This study presents a simple, useful, eco-friendly, and economical technique using doxycycline, i.e., green synthesis, to produce spherical, homogenized Ag-NPs, which are stable at room temperature for an extended period. Ag-NPs showed strong and significant antimicrobial activity. The toxicity of Ag-NPs was found to be dosage-dependent. A literature review of doxycycline-mediated Ag-NPs with significant toxic potential found few investigations. The synthesis did not include the use of toxic, hazardous chemicals; in addition, the byproducts were not toxic. The results suggest that Ag-NPs can be used safely in small dose volumes periodically as antimicrobial agents. The antimicrobial potential of Ag-NPs also indicates that they can be used to clean water bodies and other environmental features from microbial contamination in a cheap

and reproducible way. The study has limitations, as the DLS, NTA, and TEM were not utilized due to their unavailability at our institution.

CONCLUSION

We synthesized spherical, homogenized, and environmentally friendly Ag-NPs using the antibiotic doxycycline as a reducing and capping agent. The Ag-NPs were stable at room temperature for an extended period. UV-Vis, FTIR, SEM, and XRD were used to comprehensively characterize the properties of the nanoparticles. Ag-NPs showed potent antifungal activity against *C. albicans* and *C. tropicalis*. Furthermore, the toxicity assessment using mouse organs showed that lower doses of Ag-NPs had reduced toxicity. This study provides a rigorous report of toxicity evaluation of doxycycline-mediated Ag-NPs. Overall, these findings contribute to the development of a simple and cost-effective approach to synthesize less toxic Ag-NPs with promising antimicrobial properties.

ACKNOWLEDGMENTS

None.

CONFLICT OF INTEREST

The authors declare that there is no conflict of interest.

AUTHORS' CONTRIBUTION

All authors listed have made a substantial, direct and intellectual contribution to the work, and approved it for publication.

FUNDING

None.

DATA AVAILABILITY

All datasets generated or analyzed during this study are included in the manuscript.

ETHICS STATEMENT

This study was approved by the Ethical Committee, Government College University, Lahore, Pakistan.

REFERENCES

- Pathak CS, Mandal MK, Agarwala V. Synthesis and characterization of zinc sulphide nanoparticles prepared by mechanochemical route. *Superlattices Microstruct.* 2013;58:135-143. doi: 10.1016/j.spmi.2013.03.011
- Anand K, Gengan RM, Phulukdaree A, Chaturgoon A. Agroforestry waste *Moringa oleifera* petals mediated green synthesis of gold nanoparticles and their anti-cancer and catalytic activity. *J Ind Eng Chem.* 2015;21:1105-1111. doi: 10.1016/j.jiec.2014.05.021
- Zhang XF, Liu ZG, Shen W, Gurunathan S. Silver Nanoparticles: Synthesis, Characterization, Properties, Applications, and Therapeutic Approaches. *Int J Mol Sci.* 2016;17(9):1534. doi: 10.3390/ijms17091534
- Behravan M, Panahi AH, Naghizadeh A, Ziaee M, Mahdavi R, Mirzapour A. Facile green synthesis of silver nanoparticles using *Berberis vulgaris* leaf and root aqueous extract and its antibacterial activity. *Int J Biol Macromol.* 2019;124:148-154. doi: 10.1016/j.ijbiomac.2018.11.101
- Roy A, Bulut O, Some S, Mandal AK, Yilmaz MD. Green synthesis of silver nanoparticles: biomolecule-nanoparticle organizations targeting antimicrobial activity. *RSC Advances.* 2019;9(5):2673-2702. doi: 10.1039/c8ra08982e
- Patil CD, Borase HP, Patil SV, Salunkhe RB, Salunke BK. Larvicidal activity of silver nanoparticles synthesized using *Pergularia daemia* plant latex against *Aedes aegypti* and *Anopheles stephensi* and nontarget fish *Poecilia reticulata*. *Parasitol Res.* 2012;111(2):555-562. doi: 10.1007/s00436-012-2867-0
- Burdusel AC, Gherasim O, Grumezescu AM, Mogoanta L, Ficai A, Andronescu E. Biomedical Applications of Silver Nanoparticles: An Up-to-Date Overview. *Nanomaterials* (Basel). 2018;8(9):681. doi: 10.3390/nano8090681
- Lloyd-Hughes H, Shiatis AE, Pabari A, Mosahebi A, Seifalian A. Current and future nanotechnology applications in the management of melanoma: a review. *J Nanomed Nanotechnol.* 2015;6(6):1000334. doi: 10.4172/2157-7439.1000334
- Ejaz H, Ramzan M. Determination of minimum inhibitory concentrations of various antifungal agents in clinical isolates of *Candida* species. *J Pak Med Assoc.* 2019;69(8):1131-1135.
- Worth LJ, Blyth CC, Booth DL, et al. Optimizing antifungal drug dosing and monitoring to avoid toxicity and improve outcomes in patients with haematological disorders. *Intern Med J.* 2008;38(6b):521-537. doi: 10.1111/j.1445-5994.2008.01726.x
- Qureshi R, Qamar MU, Shafique M, et al. Antibacterial efficacy of silver nanoparticles against metallo- β -lactamase (*bla_{NDM}*, *bla_{VIM}*, *bla_{OXA}*) producing clinically isolated *Pseudomonas aeruginosa*. *Pak J Pharm Sci.* 2021;34(1-Suppl):237-243.
- Mathur P, Jha S, Ramteke S, Jain NK. Pharmaceutical aspects of silver nanoparticles. *Artif Cells Nanomed Biotechnol.* 2018;46(sup1):115-126. doi: 10.1080/21691401.2017.1414825
- Asgary V, Shoari A, Baghbani-Arani F, et al. Green synthesis and evaluation of silver nanoparticles as adjuvant in rabies veterinary vaccine. *Int J Nanomedicine.* 2016;11:3597-605. doi: 10.2147/ijn.S109098
- Selvaraj M, Pandurangan P, Ramasami N, Rajendran SB, Sangilimuthu SN, Perumal P. Highly potential antifungal activity of quantum-sized silver nanoparticles against *Candida albicans*. *Appl Biochem Biotechnol.* 2014;173(1):55-66. doi: 10.1007/s12010-014-0782-9
- Prabhu S, Poulouse EK. Silver nanoparticles: mechanism of antimicrobial action, synthesis, medical applications, and toxicity effects. *Int Nano Lett.* 2012;2(1):1-10. doi: 10.1186/2228-5326-2-32
- Budama-Kilinc Y, Cakir-Koc R, Zorlu T, et al. Assessment of nano-toxicity and safety profiles of silver nanoparticles. *IntechOpen.* 2018. doi: 10.5772/intechopen.75645
- Park MVDZ, Neigh AM, Vermeulen JP, et al. The effect of particle size on the cytotoxicity, inflammation, developmental toxicity and genotoxicity of silver nanoparticles. *Biomaterials.* 2011;32(36):9810-9817. doi: 10.1016/j.biomaterials.2011.08.085
- Abou El-Nour KMM, Eftaiha A, Al-Warthan A, Ammar RAA. Synthesis and applications of silver nanoparticles. *Arab J Chem.* 2010;3(3):135-140. doi: 10.1016/j.arabjc.2010.04.008
- Raveendran P, Fu J, Wallen SL. Completely "green" synthesis and stabilization of metal nanoparticles. *J Am Chem Soc.* 2003;125(46):13940-13941. doi: 10.1021/ja029267j
- Peng H, Yang A, Xiong J. Green, microwave-assisted synthesis of silver nanoparticles using bamboo hemicelluloses and glucose in an aqueous medium. *Carbohydr Polym.* 2013;91(1):348-355. doi: 10.1016/j.carbpol.2012.08.073
- Kalishwaralal K, Deepak V, Ramkumarpanthian S, Nellaiah H, Sangiliyandi G. Extracellular biosynthesis of silver nanoparticles by the culture supernatant of *Bacillus licheniformis*. *Mater Lett.* 2008;62(29):4411-4413. doi: 10.1016/j.matlet.2008.06.051
- Singh H, Du J, Singh P, Yi TH. Ecofriendly synthesis of silver and gold nanoparticles by *Euphrasia officinalis* leaf extract and its biomedical applications. *Artif Cells Nanomed Biotechnol.* 2018;46(6):1163-1170. doi: 10.1080/21691401.2017.1362417
- Al-Otibi FO, Yassin MT, Al-Askar AA, Maniah K. Green Biofabrication of Silver Nanoparticles of Potential Synergistic Activity with Antibacterial and Antifungal Agents against Some Nosocomial Pathogens. *Microorganisms.* 2023;11(4):945. doi: 10.3390/microorganisms11040945
- Qamar MU, Saleem S, Arshad U, et al. Antibacterial efficacy of Manuka honey against New Delhi Metallo- β -Lactamase producing Gram negative bacteria isolated from blood cultures. *Pak J Zool.* 2017;49(6):1997-2003. doi: 10.17582/journal.pjz/2017.49.6.1997.2003
- Chowdhury S, Yusof F, Faruck MO, Sulaiman N. Process optimization of silver nanoparticle synthesis using response surface methodology. *Procedia Eng.* 2016;148:992-999. doi: 10.1016/j.proeng.2016.06.552
- Nakamura S, Sato M, Sato Y, et al. Synthesis and Application of Silver Nanoparticles (Ag NPs) for the

- Prevention of Infection in Healthcare Workers. *Int J Mol Sci.* 2019;20(15):3620. doi: 10.3390/ijms20153620
27. Isa N, Osman MS, Abdul Hamid H, Inderan V, Lockman Z. Studies of surface plasmon resonance of silver nanoparticles reduced by aqueous extract of shortleaf spiked edge and their catalytic activity. *Int J Phytoremediation.* 2023;25(5):658-669. doi: 10.1080/15226514.2022.2099345
28. Varadavenkatesan T, Selvaraj R, Vinayagam R. Green synthesis of silver nanoparticles using *Thunbergia grandiflora* flower extract and its catalytic action in reduction of Congo red dye. *Materials Today: Proceedings.* 2020;23(1):39-42. doi: 10.1016/j.matpr.2019.05.441
29. Rozhin A, Batasheva S, Kruchkova M, Cherednichenko Y, Rozhina E, Fakhruллин R. Biogenic Silver Nanoparticles: Synthesis and Application as Antibacterial and Antifungal Agents. *Micromachines* (Basel). 2021;12(12):1480. doi: 10.3390/mi12121480
30. Ali SG, Jalal M, Ahmad H, et al. Green Synthesis of Silver Nanoparticles from *Camellia sinensis* and Its Antimicrobial and Antibiofilm Effect against Clinical Isolates. *Materials.* 2022;15(19):6978. doi: 10.3390/ma15196978
31. Leong CY, Wahab RA, Lee SL, Ponnusamy VK, Chen YH. Current perspectives of metal-based nanomaterials as photocatalytic antimicrobial agents and their therapeutic modes of action: A review. *Environ Res.* 2023;227:115578. doi: 10.1016/j.envres.2023.115578
32. Shah MZ, Guan ZH, Din AU, et al. Synthesis of silver nanoparticles using *Plantago lanceolata* extract and assessing their antibacterial and antioxidant activities. *Sci Rep.* 2021;11(1):20754. doi: 10.1038/s41598-021-00296-5
33. Kadam NS, Shelke DB, Naik AA, Tak RD, Doshi PJ, Nikam TD. Sunlight and microwave catalyzed comparative biosynthesis of silver nanoparticles using *in-vitro* and *in-vivo* biomass of *Fagonia schweinfurthii* Hadidi, its antibacterial activity and phytotoxicity. *Plant Nano Biol.* 2024;8:100071. doi: 10.1016/j.plana.2024.100071
34. Rizwana H, Alwhibi MS, Al-Judaie RA, Aldehaish HA, Alsaggabi NS. Sunlight-Mediated Green Synthesis of Silver Nanoparticles Using the Berries of *Ribes rubrum* (Red Currants): Characterisation and Evaluation of Their Antifungal and Antibacterial Activities. *Molecules.* 2022;27(7):2186. doi: 10.3390/molecules27072186
35. Tang J, Xiong L, Wang S, et al. Distribution, translocation and accumulation of silver nanoparticles in rats. *J Nanosci Nanotechnol.* 2009;9(8):4924-4932. doi: 10.1166/jnn.2009.1269
36. Hussain SM, Hess KL, Gearhart JM, Geiss KT, Schlager JJ. *In vitro* toxicity of nanoparticles in BRL 3A rat liver cells. *Toxicol In Vitro.* 2005;19(7):975-983. doi: 10.1016/j.tiv.2005.06.034
37. Foldbjerg R, Dang DA, Autrup H. Cytotoxicity and genotoxicity of silver nanoparticles in the human lung cancer cell line, A549. *Arch Toxicol.* 2011;85(7):743-750. doi: 10.1007/s00204-010-0545-5
38. Haase A, Tentschert J, Jungnickel H, et al. Toxicity of silver nanoparticles in human macrophages: uptake, intracellular distribution and cellular responses. *J Phys Conf Ser.* 2011;304(1):012030. doi: 10.1088/1742-6596/304/1/012030